PROCEEDINGS OF SCIENCE

Compton-Induced γ-ray Cascade Emissions from Blazar-type Galaxies

Mfuphi Ntshatsha,[a,*] **Markus Böttcher**[b] **and Soebur Razzaque**[a]

[a] *Centre for Astro-Particle Physics, Department of Physics, University of Johannesburg, Auckland Park Kingsway Campus, Johannesburg, 2006, South Africa*

[b] *Centre for Space Research, North-West University, Potchefstroom, 2520, South Africa*

E-mail: mfuphin95@gmail.com, Markus.Bottcher@nwu.ac.za, srazzaque@uj.ac.za

Blazars are powerful sources of high-energy (HE, $\gtrsim$ 100 MeV) to very high-energy (VHE, $\gtrsim$ 100 GeV) γ-ray emissions. According to the unified scheme for radio-loud active galactic nuclei (AGNs) radio galaxies are the parent class of the blazar population. Naturally one would expect radio galaxies, as the parent population of blazars, to be intrinsic HE and possibly VHE γ-ray emitters. This was confirmed by recent VERITAS, MAGIC and HESS detections. Previous works found that secondary electron/positron pairs can become efficiently isotropized by mild magnetic fields in AGN environments, leading to off-axis HE–VHE γ-ray cascades. We extend this work by including a more realistic Shakura-Sunyaev (SS) accretion disk model, in addition to the isotropic external radiation fields considered in previous works. We present the preliminary results of the interplay between two external radiation fields, namely the broad-line region and UV emission from the SS accretion disk, and then discuss future developments for this work.

High Energy Astrophysics in Southern Africa 2023 (HEASA 2023)
September 5 - 9, 2023
Mtunzini, KwaZulu-Natal, South Africa

*Speaker

PoS(HEASA2023)014

1. Introduction

Active galactic nuclei radiate throughout the electromagnetic spectrum. Blazars, a subclass of AGNs, are especially powerful emitters of HE–VHE γ-ray radiation. There are a number of radiative mechanisms responsible for the emissions in different frequency bands in these objects, such as inverse-Compton (IC) scattering in the γ-ray band [1–3]. In accordance with the unified scheme for radio-loud AGNs presented by [4], we assume that radio galaxies are the parent class of the blazar population. Under this assumption, one would expect radio galaxies to be intrinsic HE and possibly VHE γ-ray emitters. However, the misaligned radio galaxies were not detected in the HE γ-rays by early-generation instruments. This expectation was confirmed by recent VERITAS, MAGIC and HESS detections ([5, 6] and references therein). Typical modelling of blazar spectral energy distributions (SEDs) strongly suggests that their low frequency radiation is a consequence of synchrotron radiation by relativistic electrons, while some of the X-ray to γ-ray emission is produced by IC scattering of external low frequency radiation fields by these same electrons (e.g. [2]).

In their works [6–8] developed a Monte-Carlo code that follows the propagation of individual HE–VHE γ-rays and secondary electrons and positrons. Their initial code excluded the contribution from the accretion disk radiation on the basis of its negligible density at the "injection" height of the primary γ-rays [8]. Despite this simplification their results showed that the secondary electron/positron ($e^{\pm}$) pairs become efficiently isotropized by rather modest magnetic fields in AGN environments leading to off-axis HE–VHE γ-ray cascades. We extend this work by including a more realistic Shakura-Sunyaev accretion disk model [9], in addition to the isotropic external radiation fields already considered by [6–8]. In the following section we describe our code modifications. In the next, we present the preliminary results of the interplay between two external radiation fields, namely the broad-line region (BLR) and ultraviolet emission from the SS accretion disk. Finally, we summarise and discuss future developments for this work.

2. Code Description

In a real scenario there is no simple way to predict the interactions, trajectories and paths followed by γ-rays and $e^{\pm}$ pairs in AGN jets. For non-deterministic systems, models that are best suited to describe them are those that harness stochastic methods. The authors of [6–8] therefore developed a Monte-Carlo (MC) code to simulate Compton-induced γ-ray cascades in AGN environments. All calculations are done in the AGN frame.

Figure 1 outlines the MC cascade simulation. At the start of this simulation a γ-ray of dimensionless energy $\epsilon_\gamma \left(\equiv E_\gamma/(m_e c^2)\right)$ is randomly drawn from a power-law distribution with index $\alpha = 2.5$, where c is the speed of light in vacuum and m_e is the electron rest mass. The initial state of every primary γ-ray is assumed as follows: i) It initially propagates along the direction of the jet (defined as the z-axis), i.e. initially $\mu_\gamma \equiv \cos\theta_\gamma = 1$, where θ_γ is the angle of the γ-ray's propagation with respect to the positive z-axis. ii) It begins its trajectory at fixed coordinates $\vec{R}_0^\gamma = (x_0^\gamma, y_0^\gamma, z_0^\gamma) = (0, 0, 0.9R_{ext})$, where R_{ext} is the radius of the extent of the region in which the BLR radiation field is present.

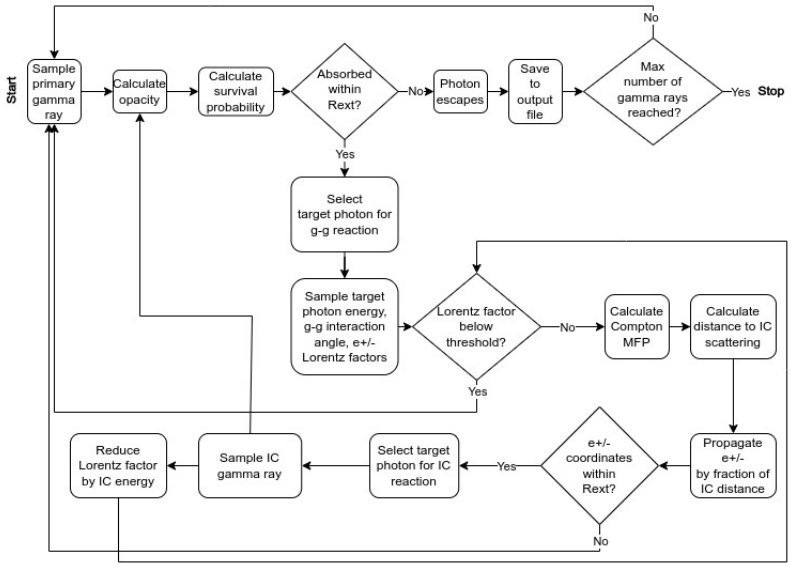

Figure 1: Schematic outlining the cascade simulation.

2.1 Monte-Carlo Routine

The only interaction we consider for γ-rays is $\gamma - \gamma$ pair production with either a BLR or accretion disk photon. In the trivial case a γ-ray does not interact with either soft photon, in which case it simply escapes. The dimensionless energy ϵ_γ, statistical weight $w_\gamma \equiv 1/(\epsilon^*_\gamma)^2$, angle cosine μ_γ, azimuthal angle ϕ_γ and time of escape t_{esc} of such a photon are saved to an output file. The energy ϵ^*_γ is that of the *primary* γ-ray that either escaped itself or was absorbed and led to the cascades. In the non-trivial case, as the γ-ray propagates it is absorbed by either a BLR or an accretion disk photon. This choice is governed by the relative opacities to $\gamma - \gamma$ absorption due to BLR and disk photons, in Section 2.1.1 we describe its treatment.

2.1.1 Gamma-gamma Interaction

The choice of an absorbing target photon is simulated by calculating the opacities $\kappa^d_{\gamma\gamma}, \kappa^{BLR}_{\gamma\gamma}$ due to the BLR radiation field and radiation from the accretion disk, respectively, as indicated by the total opacity per unit length $\kappa_{\gamma\gamma} = \kappa^d_{\gamma\gamma} + \kappa^{BLR}_{\gamma\gamma}$ in the second step of Figure 1. The annihilation probability of a γ-ray propagating in this environment is $1 - e^{(-\kappa_{\gamma\gamma} l_{abs})}$, where l_{abs} is its travel distance. Equating this to a random number $\zeta_{abs} \in (0, 1)$ and solving for l_{abs} gives the actual distance the γ-ray will travel to an absorption event. If the location of the absorption event is outside the simulation volume of radius R_{ext}, the photon escapes and is saved to an output file, otherwise it is absorbed by either a disk or BLR photon. To simulate the absorbing photon a random number $\zeta_{\gamma\gamma} \in (0, 1)$ is generated. If $\zeta_{\gamma\gamma} \leq \kappa^d_{\gamma\gamma}/\kappa_{\gamma\gamma}$ then an accretion disk photon becomes the target, otherwise it is a BLR photon. Now we define the quantities that describe the γ-ray propagation. Figure 2 illustrates the geometry of the simulated system. At the origin is the AGN's supermassive black hole (SMBH). The position vector $\vec{R}^\gamma_0$ tracks the formation site of γ-rays. The propagation of the γ-ray is tracked by $\vec{R}_\gamma \equiv l\hat{\mathbf{k}}_\gamma$, where l is the length of its travel and $\hat{\mathbf{k}}_\gamma$ given by

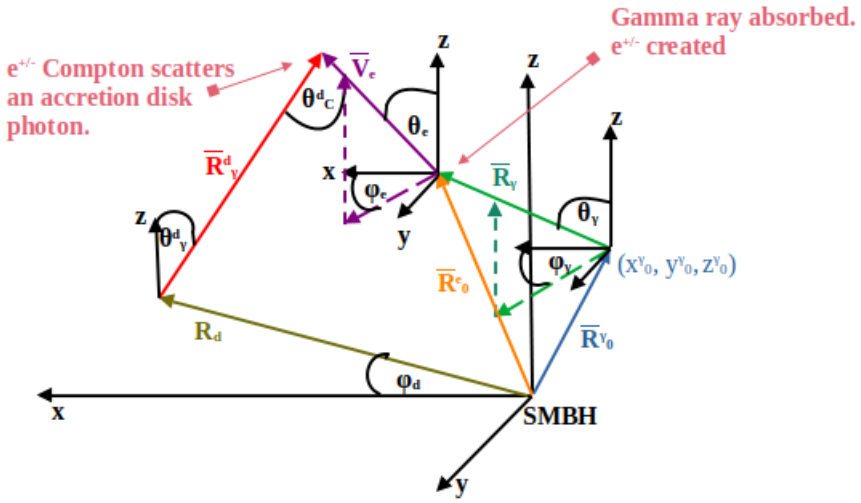

Figure 2: Full 3D geometry of γ-ray propagation simulation in AGN environment.

$$\hat{\mathbf{k}}_\gamma = \begin{pmatrix} k_x \\ k_y \\ k_z \end{pmatrix} = \begin{pmatrix} \sin\theta_\gamma \cos\phi_\gamma \\ \sin\theta_\gamma \sin\phi_\gamma \\ \cos\theta_\gamma \end{pmatrix} \tag{1}$$

is the 3 dimensional (3D) unit vector describing the γ-ray's direction of propagation. We treat the BLR radiation field as an isotropic blackbody with a temperature such that the spectrum peaks at the energy of the Lyα line. The thermal radiation from the SS accretion disk is anisotropic, thus its interaction with γ-rays is direction dependent. For this reason it is necessary to know the angle between the γ-ray and disk photon during the $\gamma - \gamma$ interaction. We define the vector $\vec{R}^d_\gamma$ given by

$$\vec{R}^d_\gamma = R^d_\gamma \begin{pmatrix} \sin\theta^d_\gamma \cos\phi^d_\gamma \\ \sin\theta^d_\gamma \sin\phi^d_\gamma \\ \cos\theta^d_\gamma \end{pmatrix} = \begin{pmatrix} x^\gamma_0 + lk_x - R_d\cos\phi_d \\ y^\gamma_0 + lk_y - R_d\sin\phi_d \\ z^\gamma_0 + lk_z \end{pmatrix} \tag{2}$$

that describes an accretion disk photon's distance, R_d, from the black hole and direction travelled on its way to reacting with a γ-ray. The dot product of $\vec{R}^d_\gamma$ and $\hat{\mathbf{k}}$ gives their interaction angle cosine $\mu^d_{\gamma\gamma} \equiv (\vec{R}^d_\gamma \cdot \hat{\mathbf{k}}_\gamma)/(R^d_\gamma)$.

With these quantities we are ready to calculate the opacity $\kappa^d_{\gamma\gamma}$ of a photon with dimensionless energy ϵ_γ due to the accretion disk radiation as

$$\kappa^d_{\gamma\gamma} = \int_{R_{in}}^{R_{out}} R_d\, dR_d \int_0^{2\pi} d\phi_d \int_0^\infty d\epsilon \frac{dn_{ph}}{dA_d d\epsilon}(1-\mu^d_{\gamma\gamma})\sigma_{\gamma\gamma}(\epsilon_\gamma, \epsilon, \mu^d_{\gamma\gamma}) \tag{3}$$

$$\frac{dn_{ph}}{dA_d d\epsilon} = \frac{45}{2}\frac{\sigma_{SB}}{\pi^5}\frac{(m_e c^2)^3}{c k_B^4}\frac{|\cos\theta^d_\gamma|}{(R^d_\gamma)^2}\frac{\epsilon^2}{\exp[\epsilon/\Theta(R_d)]-1} \tag{4}$$

where $dn_{ph}/dA_d d\epsilon$ is the accretion disk radiation field, σ_{SB} is the Stefan-Boltzmann constant, k_B is Boltzmann's constant, $\sigma_{\gamma\gamma}$ is the $\gamma - \gamma$ cross-section and $\Theta(R_d) \equiv k_B T(R_d)/(m_e c^2)$ [1] is the accretion disk's radially dependent dimensionless temperature. Quantities related with the BLR are

implemented in the code as described in [6]. In this paper we only show calculations of quantities related with the SS accretion disk. From here, depending on whether the target photon is a BLR or accretion disk photon, its energy and direction are sampled as illustrated in Figure 1. These, together with ϵ_γ, are then used to sample the Lorentz factors $\gamma_\pm$ of the subsequent $e^\pm$ pair.

2.1.2 Inverse-Compton Interaction

The coordinates of absorption of a γ-ray become the initial coordinates of both $e^\pm$. Its energy ϵ_γ is divided into $\gamma_\pm$ as described in [6], and then the $e^\pm$ are tracked individually. The inverse Compton mean-free-path (MFP) length λ_C^{-1} of an $e^{-(+)}$ of Lorentz factor $\gamma_{-(+)}$ is then calculated for propagation in the BLR and in the accretion disk radiation fields. In analogy to the selection procedure described in Section 2.1.1, the target photon for Compton up-scattering is selected. In place of opacities, $(\lambda_C^{d,BLR})^{-1}$ are used rather, where the inverse Compton MFP length of an $e^{-(+)}$ in the accretion disk radiation field $(\lambda_C^d)^{-1}$ is given by

$$(\lambda_C^d)^{-1}(\gamma_{-(+)}) = \int_{R_{in}}^{R_{out}} R_d\, dR_d \int_0^{2\pi} d\phi_d \int_0^\infty d\epsilon \frac{dn_{ph}}{dA_d d\epsilon}(1-\beta\mu_C^d)\sigma_C(\epsilon, \gamma_{-(+)}, \mu_C^d) \quad (5)$$

where $\beta = \sqrt{1-(\gamma_{-(+)})^{-2}}$, $\mu_C^d \equiv (\vec{R}_\gamma^d \cdot \vec{V}_e(\Delta t))/(R_\gamma^d V_e(\Delta t))$ is the Compton interaction angle cosine with a disk photon, σ_C is the Compton cross-section and $\vec{V}_e(\Delta t)$ defined in Figure 2 is the $e^{-(+)}$'s velocity in a time interval Δt. The pairs gyrate in a uniform magnetic field $\vec{B} = (B_x, B_y, B_z)$, and the code calculates their positions by solving their Euler-Lagrange equations. The solutions to these equations trace out helical paths. We choose Δt such that the distance travelled by particles is a fraction of the helical path, re-evaluating the Compton MFP length every Δt. This approximates a tangential line segment along the path, whose direction becomes that of the outgoing secondary γ-ray. The particle is tracked like this until it either escapes the simulation volume of interest or its energy becomes too low to produce a γ-ray. For every secondary γ-ray produced at time Δt, its initial coordinates, $\vec{R}_0^\gamma$, are set to the coordinates of its production site before it is tracked with the same routine as the primary γ-rays.

3. Preliminary Results

We analyse the output file data in a separate post-processing routine that produces spectra and light curves. Figure 3 shows the cascade spectra (*left*) and light curves (*right*) for an AGN containing a supermassive black hole of mass 10^8 $M_\odot$. The left panel shows the spectra as viewed from five equal-sized angle cosine bins in the range $-1 \leq \mu \leq 1$, while the right panel shows light curves of five equal-sized energy bins in the range 10 MeV $\leq E \leq$ 10 TeV. These light curves show the variability of the AGN's cascade emission as seen by observers whose line of sight falls within $36° < \theta_{obs} < 60°$ with respect to the jet axis. The parameters considered in our simulations, namely magnetic field $\vec{B}$, BLR radiation energy density u_{BLR} and BLR size R_{ext} fall within the ranges performed by [6, 11]. The magnetic field in this AGN's environment is $(B_x, B_y, B_z) = (0, 0.1, 1)$ mG. Its nucleus is surrounded by a broad-line region with $u_{BLR} = 5 \times 10^{-2}$ erg/cm^3. The BLR can reprocess and re-emit 10% of the accretion disk radiation [2, 10]. Then this BLR energy density

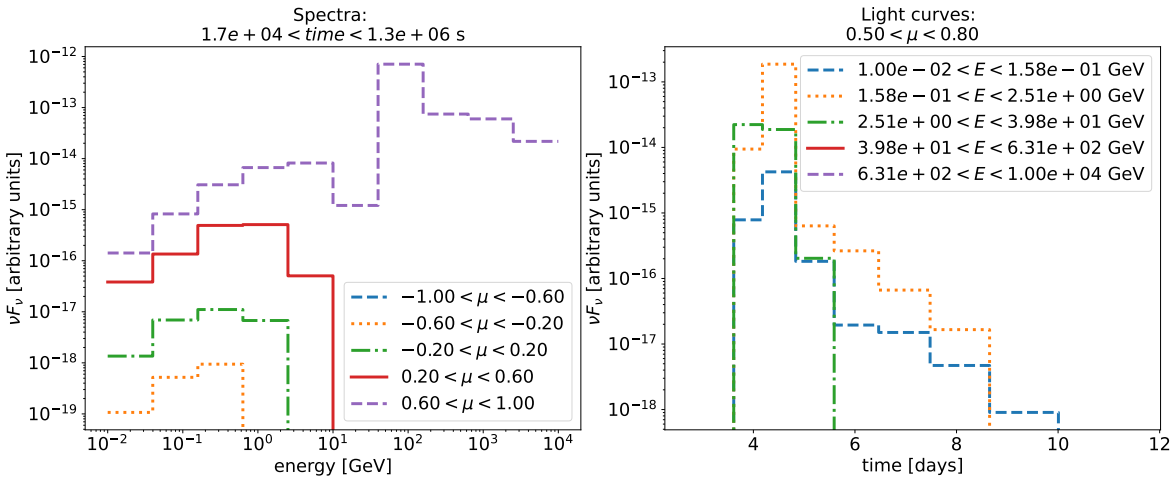

Figure 3: Spectra and light curves of an AGN with a black hole mass of $10^8 M_\odot$ and an accretion disk luminosity of 1.9×10^{43} erg/s. On the *left* are the AGN's cascade spectra in five equal-sized angle cosine bins, and on the *right* are its light curves in five equal-sized energy bins.

corresponds to an accretion disk luminosity of $L_d = 10L_{BLR} = 10(4\pi c R_{ext}^2 u_{BLR}) = 1.9 \times 10^{43}$ erg/s. In the simulation we defined the extent of the AGN volume to have radius $R_{ext} = 10^{16}$ cm, where all the primary γ-rays are produced at $(x_0^\gamma, y_0^\gamma, z_0^\gamma) = (0, 0, 0.9R_{ext})$ in the direction described by $(\mu_\gamma, \phi_\gamma) = (1, 0)$. In the $0.6 < \mu \leq 1$ bin VHE emission is observed beginning at a time $t_0 \lessapprox 0.1(R_{ext}/c)$ from the start of the simulation, corresponding to primary γ-rays escaping the simulation volume without being absorbed. Emission at larger angles (i.e. $\mu < 0.6$) is seen from a time $\gtrsim (R_{ext}/c)$, as seen in the light curves where all emissions are seen from $(R_{ext}/c) \approx 3.86$ days. The light curves then indicate the variability timescale of the cascade emission in the angular location of a specific observer, for example $0.5 < \mu < 0.8$ in the case of Figure 3 (*right*). For a given angular location, the width of the light curves increases with decreasing cascade photon energy. This is to be expected because if a HE γ-ray is absorbed leading to a cascade, then the cascade process delays the escape time of photons from the AGN volume, while reducing the energy of the initiating photon. On the other hand, unabsorbed higher energy photons escape sooner, delayed only by light travel times from their production site to the BLR boundary. Hence an observer would see them with thinner light curve widths. This same trend was reported by [3, 11]. The widths of the light curves show $2.5 < E < 40$ GeV emission variability in the order 1 day. The cascade spectra (Figure 3, *left*) show that observers see lower-energy γ-rays with increasing viewing angles. This is because the γ-rays propagating at large angles with respect to the jet axis can interact with anisotropic disk photons at more favourable angles and become absorbed more efficiently.

4. Summary

We have set out to study the radiative signatures of radio-loud AGNs as viewed by observers at different angles with respect to the AGN jet. We modified a MC code that explores the effect of inverse-Compton supported γ-ray cascades on AGN spectra by including anisotropic radiation from a SS accretion disk model. The simulation progresses consistently, however it requires a large

computation time. Thus, for the simulation presented here we propagated only 500 primary γ-ray photons, resulting in limited photon statistics. We can improve on these by increasing the number of photons propagated. With increased number of injected primary photons, we expect to see higher resolution spectra and light curves. For example, in the spectra shown in Figure 3 photons with energies > 10 GeV are visible in a rather large angular bin ($0.6 < \mu < 1$). We note that the finer angular bin ($0.5 < \mu < 0.8$) considered in the light curves of Figure 3 is contained within the $0.6 < \mu < 1$. However, the reduced photon statistics do not reveal the light curve corresponding to these > 10 GeV photons, particularly the $E > 40$ GeV photons. Despite insufficient photon statistics the simulation has produced results consistent with [11] when we performed a similar study looking at the time-dependence of the γ-ray cascades, as seen in the light curve of Figure 3. Furthermore, the significance of absorption by accretion disk radiation increases with decreasing R_{ext}. The emphasis of the current work was on describing the modifications made on the code and demonstrating its consistency. Future works will focus more on in-depth analyses of the cascade emission. These studies will then be compared with observational data of some blazars and misaligned radio-loud active galaxies. We note that although the choice of $z_0^\gamma = 0.9R_{ext}$ is arbitrary, the origin of primary γ-rays has to be sufficiently far from the central black hole, otherwise if they are produced too deep within (e.g. if the simulation is started with $z_0^\gamma < 0.5R_{ext}$) they would all be absorbed and not observed within the cone of the jet, which is inconsistent with the blazar class.

References

[1] M. Böttcher, H. Mause and R. Schlickeiser, *γ-ray emission and spectral evolution of pair plasmas in AGN jets. I. General theory and a prediction for the GeV - TeV emission from ultrarelativistic jets.*, *A&A* **324** (1997) 395 [astro-ph/9604003].

[2] G. Ghisellini and F. Tavecchio, *Canonical high-power blazars*, *MNRAS* **397** (2009) 985.

[3] J. Sitarek and W. Bednarek, *Time-dependent gamma-ray production in the anisotropic inverse Compton $e^{+/-}$ pair cascade initiated by electrons in active galaxies*, *MNRAS* **409** (2010) 662 [1004.0172].

[4] C. M. Urry and P. Padovani, *Unified schemes for radio-loud active galactic nuclei*, *PASP* **107** (1995) 803.

[5] C. D. Dermer and B. Giebels, *Active galactic nuclei at gamma-ray energies*, *CRP* **17** (2016) 594.

[6] P. Roustazadeh and M. Böttcher, *Very high energy gamma-ray-induced pair cascades in blazars and radio galaxies: Application to NGC 1275*, *ApJ* **717** (2010) 468.

[7] P. Roustazadeh and M. Böttcher, *Very high energy gamma-ray-induced pair cascades in the radiation fields of dust Tori of active galactic nuclei: Application to Cen A*, *ApJ* **728** (2011) 134.

[8] P. Roustazadeh and M. Böttcher, *Synchrotron Emission from Very High Energy Gamma-Ray-induced Pair Cascades in Active Galactic Nucleus Environments*, *ApJ* **750** (2012) 26 [1202.6084].

[9] N. I. Shakura and R. A. Sunyaev, *Black holes in binary systems. observational appearance.*, *A&A* **24** (1973) 337.

[10] G. Ghisellini and P. Madau, *On the origin of the gamma-ray emission in blazars*, **280** (1996) 67.

[11] P. Roustazadeh, S. Ghrush and M. Böttcher, *Time-Dependence of VHE gamma-ray induced Pair Cascades in AGN Environments*, in *3rd Annual Conference on High Energy Astrophysics in Southern Africa (HEASA2015)*, p. 18, Jan., 2015, DOI.